Heliyon

Received:
29 November 2016
Revised:
3 February 2017
Accepted:
13 March 2017

Cite as: Lara A. Thompson, Csilla Haburcakova, Richard F. Lewis. Postural compensation strategy depends on the severity of vestibular damage.
Heliyon 3 (2017) e00270.
doi: 10.1016/j.heliyon.2017.e00270

Postural compensation strategy depends on the severity of vestibular damage

Lara A. Thompson [a,b,*], **Csilla Haburcakova** [a], **Richard F. Lewis** [a,b,c]

[a] *Jenks Vestibular Physiology Laboratory, Massachusetts Eye and Ear Infirmary, 243 Charles Street, Boston, MA 02114, USA*

[b] *Harvard- MIT Health Sciences and Technology, 77 Massachusetts Avenue, E25-519, Cambridge, MA 02139, USA*

[c] *Department of Otology and Laryngology, Harvard Medical School, 243 Charles Street Boston, MA 02114, USA*

* Corresponding author at: School of Engineering and Applied Sciences, Department of Mechanical Engineering, University of the District of Columbia, 4200 Connecticut Avenue NW, 42-213F, Washington DC 20008, USA.
E-mail address: lthomps@alum.mit.edu (L.A. Thompson).

Abstract

The purpose of this study was to investigate the effects of various levels of vestibular function on balance in two, free-standing rhesus monkeys. We hypothesized that postural control strategy depended on the severity of vestibular damage. More specifically, that increased muscle stiffness (via short-latency mechanisms) was adequate to compensate for mild damage, but long-latency mechanisms must be utilized for more severe vestibular damage.

One animal was studied for pre-ablated and mild vestibular dysfunction states, while a second animal was studied in a pre-ablated and severe vestibular dysfunction state. The vestibulo-ocular reflex (VOR), an eye movement reflex directly linked to vestibular function, was used to quantify the level of vestibular damage. A postural feedback controller model, previously only used for human studies, was modified to interpret non-human primate postural responses (differences observed in the measured trunk roll) for these three levels of vestibular function. By implementing a feedback controller model, we were able to further interpret our empirical findings and model results were consistent with our above hypothesis. This study establishes a baseline for future studies of non-human primate posture.

http://dx.doi.org/10.1016/j.heliyon.2017.e00270

Keywords: Health sciences, Biomedical engineering, Physiology

1. Introduction

Adequate balance is necessary to perform daily activities and to avoid falls. Eight million American adults have chronic balance impairments due to damage in the peripheral vestibular system [1]. Many patients with vestibular dysfunction will experience blurred vision (or oscillopsia), a perceived spinning sensation (or vertigo), and imbalance. Unfortunately, vestibular loss sufferers are receiving reduced sensory information necessary to maintain their balance [2, 3]. The seemingly simple task of standing involves complex interactions of the sensorimotor system (i.e., the integration of inputs to the visual, somatosensory, and vestibular systems). When healthy individuals perform balance activities encountered in daily-living situations (e.g., walking on an uneven surface in the dark or standing with a narrowed stance) they are able to maintain their balance with minimal difficulty. However, for these common balance situations, individuals suffering from severe vestibular dysfunction have loss of equilibrium that can cause unsteady balance leading to falls. Although imbalance is a major concern, little is known regarding compensation mechanisms in individuals suffering from the range of mild to marked vestibular impairments.

In our previous study [4], we investigated postural stability during head turns for two rhesus monkeys: one animal study contrasted normal and mild bilateral vestibular ablation and a second animal study contrasted severe bilateral vestibular ablation with and without prosthetic stimulation from an invasive vestibular prosthesis. However, here we examine the effects of the postural compensation, which the animal develops on one's own, for different levels of peripheral vestibular dysfunction. Since trunk roll is correlated with fall risk [5], we focused on trunk stability for rotations about an earth-horizontal axis (i.e., our focus was on trunk roll).

We hypothesized that an animal with mild vestibular damage would be able to stabilize its posture, but that an animal suffering from severe vestibular damage would become unstable (i.e., exhibit larger trunk roll). Previous research has shown that postural stability during quiet stance (i.e., standing in the absence of voluntary movements or external perturbations) in vestibulopathic subjects is affected by the: a) base-of-support [3, 6]; b) support surface characteristics [7]; and c) non-weight bearing sensory cues (or "light touch") [8]. Here, we examined how each of these affected postural stability in monkeys when they were in a pre-ablated state or following either mild or severe peripheral vestibular ablation.

For further interpretation of physiologic mechanisms used to compensate for loss of vestibular function, our experimental findings were simulated using a quiet stance feedback controller model. Although feedback controller models have been

http://dx.doi.org/10.1016/j.heliyon.2017.e00270

employed to study human balance with the body represented as a single link inverted pendulum controlled by a proportional-integral-derivative (PID) controller (e.g., [9, 10, 11, 12, 13]), very little (if any) has been published on applying these models to predict and characterize postural control non-human primate animal subjects. Quantitative animals models are needed to capture the neurophysiological and biomechanical effects of balance disorders, as well as responses to novel rehabilitative solutions that cannot yet be conducted in humans.

Our model results, the first of their kind, suggest that dysfunction caused by mild vestibular ablation was overcome by increasing muscle stiffness [7, 14] that reduced the effects of external perturbations without compromising speed, accuracy or precision (e.g., [15, 16, 17]). Spinal reflexes generate rapid, short-latency contractions that can compensate for small movements. For larger trunk rolls when vestibular ablation was severe, long-latency mechanisms were employed (e.g., [18]). To the best of our knowledge, this is the first study of postural control in non-human primates for: platform configurations involving varied base-of-support and support surface cues; different levels of vestibular function; and using a feedback controller model to explain the rhesus monkey postural responses.

2. Methods

Experiments were approved by the Institutional Animal Care and Use Committee and were in accordance with USDA guidelines. Two juvenile female rhesus monkeys were used: monkey S (7.9 kg) and monkey M (6.7 kg). Monkey "S" was studied in a state of *Severe* vestibular damage and monkey "M" was studied in a state of *Mild* vestibular damage. Vestibular ablation was accomplished by intra-tympanic (IT) gentamicin and systemic intramuscular (IM) streptomycin injections [19]. Monkey S received 3 cycles of bilateral IT gentamicin followed by two cycles of IM streptomycin (same dosage of 350 mg/kg/day for 21 days); monkey M received 6 cycles of bilateral IT gentamicin followed by 3 cycles of IM streptomycin using the same dosages. The vestibulo-ocular reflex (VOR), used to quantify the level of vestibular function, was measured with a CNC search coil system [20]. A head-bolt immobilized the head during VOR testing and held the tubing in the head-fixed reward system. In both animals, peripheral vestibular damage was assessed by measuring the VOR during en bloc head and body sinusoidal roll rotation of 0.5 Hz about an earth-horizontal axis. Monkey M had only a slight reduction in vestibular function (roll VOR gain was only mildly reduced by 21% (0.42 → 0.33)). It was observed that Monkey M was more resistant to the aminoglycocide treatments. However, monkey S had more a severe ablation (roll VOR gain dropping by 60% (0.58 → 0.23)). Although it was not the focus of our balance study presented here, the finding that one animal was more resistant to aminoglycocides than the other, as observed from the VOR, was

http://dx.doi.org/10.1016/j.heliyon.2017.e00270

interesting and unexpected. The VOR is a functional test that estimates well the degree of compensation between the two vestibules, but the precision of the compensation mechanisms could be different according to the level of anatomical lesion. We were unable to utilize other measures (e.g., caloric testing) in both animals to further observe vestibular ablation, and acknowledge that this was a limitation. However, to the best of our knowledge and observation from our gathered VOR measures, one animal (monkey S) had a higher level of ablation than the other (monkey M). Although the extent to which the lesion was bilateral was unknown, the aminoglycoside lesion was presumed to affect both ears equally. As previously stated, the primary goal of our study to examine the postural effects of mild versus severe vestibular ablation and not eye movements, per se.

2.1. Balance platform and training

Fig. 1 shows a schematic of the balance platform. The medial-lateral stance width between the footplates was set at 18 cm ("wide") or 9 cm ("narrow"). The support surface of each footplate was covered with either very thin rubber ("gum") or thick compliant rubber ("foam"). The platform configurations were: gum-wide, gum-narrow, foam-wide, and foam-narrow. By varying the medial-lateral stance width, we could destabilize the monkeys in roll. Covering the support surface with either thin rubber or thick, compliant foam allowed us to control the somatosensory cues provided by the limbs. By anchoring the water reward tube to the ground or attaching it to the animal's head, we could add or remove a non-weight bearing, earth-fixed orientation cue. During the experiments, visual orientation cues were limited by black draping of the surrounding visual field and dim ambient lighting.

The water reward tube in the monkey's mouth was either connected to the platform (earth-fixed, Fig. 1) or to the animal's headcap (head-fixed). The earth-fixed reward system set-up provided a spatial orientation cue because it was attached to

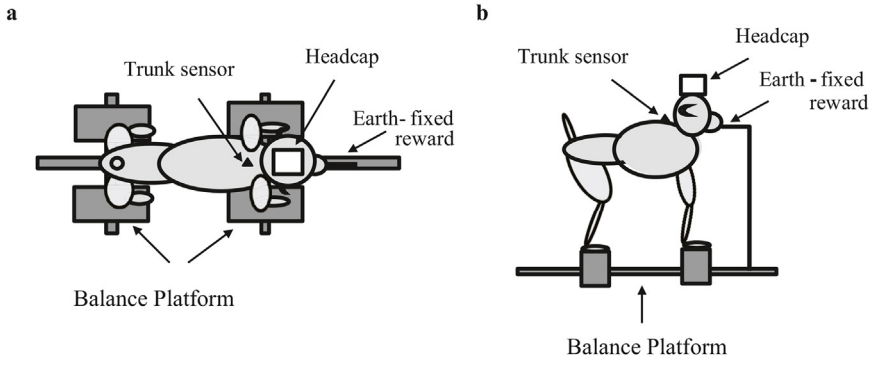

Fig. 1. Schematic illustration of a monkey standing on the balance platform, with the water reward in the earth-fixed configuration; a) top view and b) side view.

http://dx.doi.org/10.1016/j.heliyon.2017.e00270

the ground. However, the head-fixed reward system removed this cue. For each, the tubing was non-weight bearing.

The monkeys wore a vest that held a small position sensor (minibird, Ascension Co., Burlington, VT) in a mid-sagittal position at the rostral-caudal level of the scapula base (Fig. 1). Angular and linear positions were recorded at 100 Hz. Videos of the test sessions were made using infrared Kodak cameras, with the field illuminated by infrared lighting (48-LED Illuminator Light Infrared Night Vision). Data from all systems were synchronized using a timing pulse.

During training and experiments, the animal was placed on the platform by two experimenters, with each limb situated on each of the four footplates. The footplates were equipped with force sensors (ME-Meßsysteme GmbH, KD24S, Hennigsdorf, Germany), such that when over 500 grams was applied vertically to each of the four footplates, the animal was rewarded juice. Although the juice reward would cease below 500 grams, data was acquired until the experimenter manually stopped data acquisition. The animal would typically stand on the platform quietly and uninterrupted for several minutes.

2.2. Trunk roll parameters

The principal variables we analyzed were based on the roll of the trunk. Since we were interested in trunk roll deviations rather than static (mean) tilt, we quantified the root-mean-squared (RMS) trunk roll. This was done by dividing the data into 15 s segments, removing the offset, and then calculating the RMS trunk roll for each segment. An overall mean RMS roll and standard error for all 15 s segments were calculated for each platform configuration. From the trunk roll, we also quantified peak-to-peak displacement (MAXD), root-mean-square velocity (RMSV), centroid frequency (CFREQ), and frequency dispersion (FREQD) that can range from 0 to 1 (i.e., a perfect sinusoid would have a frequency dispersion of 0) [21, 22]. The trunk roll parameters are defined as follows:

Maximum distance (MAXD):

$$MAXD = \max(x(i)) - \min(x(i)) \tag{1}$$

where x(i) is position data for the trunk for sample number "i"

Root-mean-square of trunk position (RMS):

$$RMS = \sqrt{\frac{1}{N}\sum_{i=1}^{N}[x(i)]^2} \tag{2}$$

where x(i) is position data for the trunk for sample number "i"

N = number of samples

http://dx.doi.org/10.1016/j.heliyon.2017.e00270

Root-mean-square velocity (RMSV):

$$RMSV = \sqrt{\frac{1}{N-1}\sum_{i=1}^{N-1}[\dot{x}(i)]^2} \tag{3}$$

where $\dot{x}(i)$ is derivative of the position data for the trunk for sample number "i"

N = number of samples

Frequency Dispersion (FREQD):

$$FREQD = \sqrt{1 - \frac{{\mu_1}^2}{\mu_0 \times \mu_2}} \tag{4}$$

where spectral moments μ_o, μ_1, μ_2 are calculated for k = 0, 1, 2, respectively in the equation below:

$$\mu_k = \sum_{i=1}^{m}(i \times \Delta f)^k \times G(i \times \Delta f)$$

Δf is the frequency increment (computed as 1/time increment between samples)

G(i x Δf) = discrete Fourier transform of the trunk position trace where "i" is the sample number

μ_k = number of discrete power spectral density estimates

Centroid Frequency (CFREQ):

$$CFREQ = \sqrt{\frac{\mu_2}{\mu_0}} \tag{5}$$

where μ_o and μ_2 are the zeroth and second spectral moments, respectively (as described in Eq. (4)).

For the statistical analysis on the data, SigmaStat 4.0 (Systat Software Inc., San Jose, CA) was used. The Mann-Whitney test was used to compare differences between two independent groups (e.g., the effect of vestibular ablation on trunk roll). Unlike the t-test, the Mann-Whitney test does not require the assumption of normal distributions. Further, the Holm-Sidak method was used for multiple comparisons (e.g., vestibular ablation level, stance width or support surface).

2.3. Feedback controller model

To investigate the postural mechanisms used for different levels of vestibular function, we implemented a feedback controller model (Fig. 2). We modeled *only* the (bipedal) foretrunk of the animal as a simple inverted pendulum and used a similar approach to that used to model postural control in bipedal humans (e.g., [9], [21], [11, 23, 24, 25]). Furthermore, we *only* model-simulated the foam-wide

http://dx.doi.org/10.1016/j.heliyon.2017.e00270

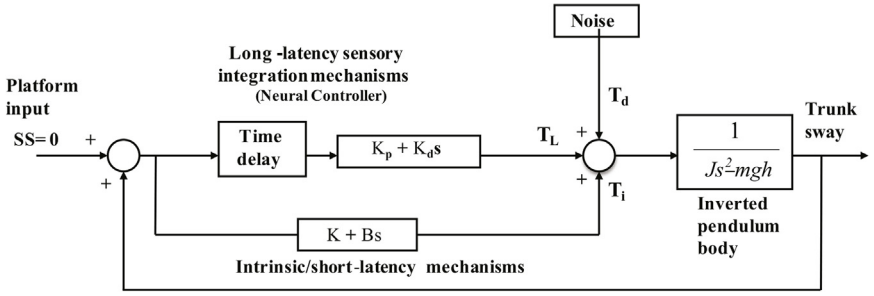

Fig. 2. Feedback controller model implemented for rhesus monkey posture.

platform configuration for the head-fixed reward system (in the absence of a "light touch" cue), where we had observed marked discrepancies between the mildly ablated and severely ablated trunk rolls.

The Maurer and Peterka [21] model described control mechanisms for human quiet stance. In this model, the platform input (SS) is zero because the platform itself is stationary. However, the mechanisms underlying spontaneous trunk roll were simulated using a disturbance torque (T_d) generated by a low-pass filtered, white-noise disturbance input. The noise block was set to have a gain of 462 N*m and the time constant was set to 100 s. We did not include the contribution of different sensory modalities (weightings) in that their sum was assumed to equal one within the model. In order to remain upright, the subject exerts a corrective torque comprised of a torque (T_L) generated by mechanisms with long-latency neural time delay, and an intrinsic/short-latency torque (T_i) generated by mechanisms with little or no time delay. We refer to intrinsic/short-latency mechanisms as those mediated by the inherent mechanical properties of the muscles and associated soft tissues around the joints and by spinal reflexes with very short neural time delays. These consist of stiffness (K) and damping (B) contributions. We refer to long-latency mechanisms as those which have latencies of >200 milliseconds and are mediated by vestibular, visual, and somatosensory inputs. The long-latency torque (T_L) is equal to the angular deviation times the long-latency stiffness (represented by K_p) and a component that is the time derivative of the angular deviation times the long-latency damping (represented by K_d). The quiet stance proportional-derivative feedback control model described above was implemented using Simulink (MATLAB, MathWorks, Natick, MA, version 2008b). Using anthropometric measurements derived from cadaveric rhesus monkeys [26], the inverted pendulum moment of inertia of the foretrunk, J, was set to 0.09 kg*m^2 and inverted pendulum mass x gravity x center-of-mass height was set to 2.5 kg*m^2/s^2. Human mean intrinsic/short-latency stiffness (~4 N*m/deg) and intrinsic/short-latency damping (~0.7 N*m*s/deg) values for small ankle stretch (0.15°) were used as initial values for the controller model [27]. Model simulations were run for 600 s, which were then segmented into forty, 15 s trials. An overall mean and standard

http://dx.doi.org/10.1016/j.heliyon.2017.e00270

error for each trunk roll parameter (MAXD, RMS, RMSV, FREQD, and CFREQ) were computed for each model simulated state and compared to the empirical parameters.

For the simulations of the pre-ablated and mildly ablated states, long-latency mechanisms were assumed to play a minimal role and set to ~0 [27]. By varying the human values of K = 4 N*m/deg and B = 0.7 N*m*s/deg, K predominantly affected the MAXD and RMS position parameters, and B predominantly affected velocity (RMSV) and frequency trunk roll measures (CFREQ and FREQD). However, to determine the optimal values for K and B, we determined the intersection between the measured RMS and RMSV values and the model-simulated RMS and RMSV curves resulting from various values for K and B. We: 1) varied K (3 to 12 N*m/deg) and B (0.3 to 1.2 N*m*s/deg); 2) determined the corresponding model-simulated output trunk roll (for each K and B value); 3) calculated the corresponding model-simulated RMS and RMSV; 4) located the K and B values for which an intersection occurred between the model-simulated and measured RMS and RMSV values. We chose the above methods because it provided more direct control over the fit quality. The optimal K and B values were based on RMS and RMSV and we computed the other model-simulated parameters (MAXD, FREQD and CFREQ) to observe that they were within ~10% of the experimental values for the head-fixed reward.

The simulations described above were conducted for only the head-fixed reward configuration (i.e., the earth-fixed reward was not interfering with the animals' postural responses) and for the foam-wide test condition, where marked differences in trunk roll were observed.

3. Results

For monkey M prior to vestibular ablation, roll did not depend significantly on stance width or support surface (Holm-Sidak, $p > 0.05$ for each) but there was a significant non-linear interaction between the width and surface of the platform (Holm-Sidak: $p < 0.001$). After mild vestibular ablation, in the "least challenging" platform configuration (gum-wide) due to available support surface cues and a wide support base, motion of the trunk about the roll axis *decreased* compared to normal (a pattern observed in four, platform configurations (Fig. 3)). The effects of vestibular ablation on trunk roll and the dependence of trunk roll on the support surface were significant (Mann-Whitney test: $p = 0.008$; Holm-Sidak: $p = 0.003$) and dependence on stance width was insignificant (Holm-Sidak: $p = 0.62$).

For monkey S prior to vestibular ablation, roll's dependence on stance width and support surface was significant (Holm-Sidak test: $p < 0.001$ for each), with a significant non-linear interaction between width and platform surface (Holm-Sidak: $p < 0.001$). After severe ablation, the motion of the trunk about the roll axis

http://dx.doi.org/10.1016/j.heliyon.2017.e00270

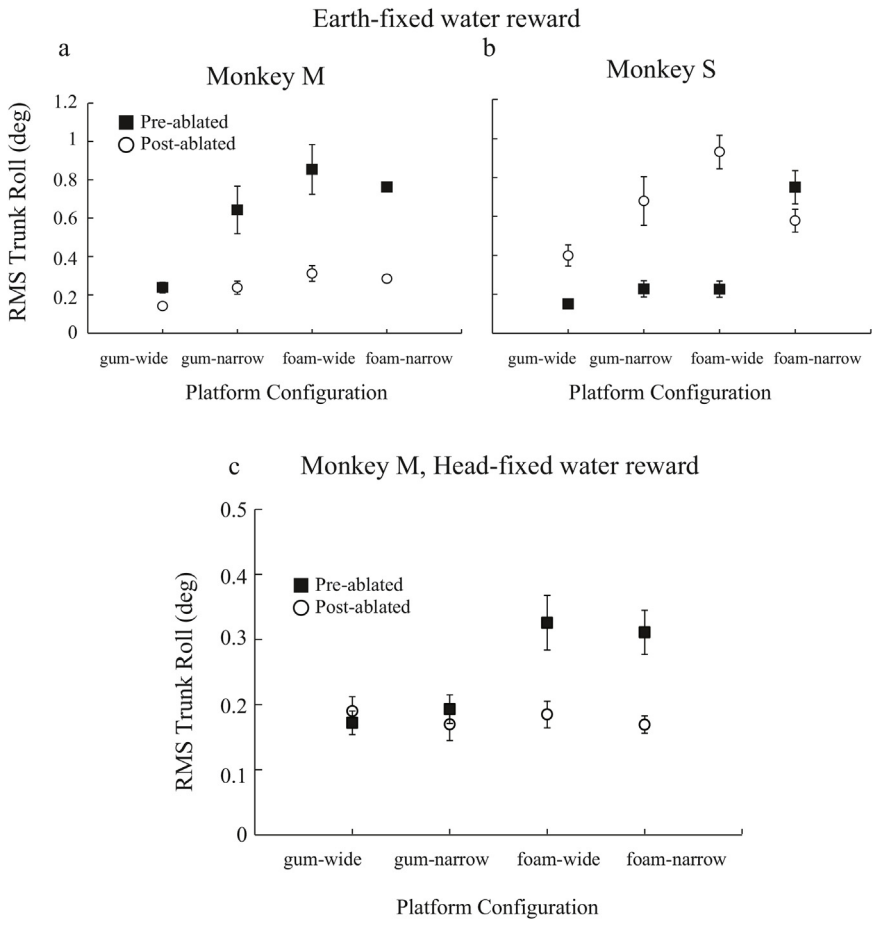

Fig. 3. (*Top)* For monkey M and monkey S: Root-mean-squared (RMS) roll tilt of the trunk prior to (black squares) and following (open circles) vestibular ablation, in the four platform configurations for the earth-fixed water reward system. Icons represent the means of 15–41, 15 s trials and error bars indicate standard error; *(Bottom)* For monkey M: Root-mean-squared (RMS) roll tilt of the trunk prior to (black squares) and following vestibular ablation (open circles), in the four platform configurations using the head-fixed water reward system. Icons are means and error bars are standard error.

increased for all platform configurations except for foam-narrow (Fig. 3). Our observations indicated that monkey S crouched closer to the platform in the most difficult (foam-narrow) condition after vestibular ablation, a postural change that lowered its center of mass leading to a reduction in trunk roll. We did not observe the same behavior in monkey M. The effect of vestibular ablation on trunk roll was significant in monkey S (Mann-Whitney test: $p < 0.001$), dependence of trunk roll on the support surface was significant (Holm-Sidak: $p = 0.02$), and dependence on stance width was insignificant (Holm-Sidak: $p = 0.68$).

Our analysis described above involved the use of the earth-fixed reward system. However, when the water reward tube was earth-fixed, it may have provided an

http://dx.doi.org/10.1016/j.heliyon.2017.e00270

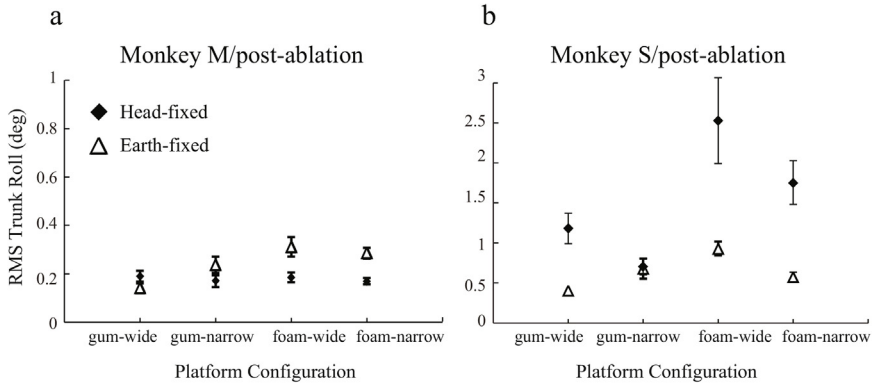

Fig. 4. RMS trunk roll for both monkeys post-vestibular ablation, in the four platform configurations, with (earth-fixed water reward, open triangles) and without (head-fixed water reward, black diamonds) the "light touch" sensory cue. Note differences in y-axis scale.

additional, non-weight bearing sensory signal about head orientation relative to the support surface. When the reward was mounted directly on the monkey's head cap (head-fixed), this additional cue was removed. Monkey M was studied using both the earth-fixed and head-fixed rewards for all platform configurations, pre and post-ablation. Fig. 3 (bottom) shows the RMS roll tilt for monkey M using the head-fixed reward. For both reward conditions (Fig. 3), trunk roll generally increased in the pre-ablated state as the platform configuration became more difficult, and following ablation trunk roll amplitudes decreased overall (head-fixed/pre-ablation = 0.25 deg/s, head-fixed/post-ablation = 0.18 deg/s, Mann-Whitney $p = 0.002$; earth-fixed/pre-ablation = 0.45 deg/s, earth-fixed/post-ablation = 0.23 deg/s, Mann-Whitney $p = 0.008$). The principal differences between the two water reward conditions were the presence of larger trunk roll magnitudes pre-ablation when the earth-fixed reward was used and the larger increase in trunk roll produced by narrowing the platform with the gum rubber surface in the pre-ablated state.

In order to evaluate how the earth-fixed, non-weight bearing orientation information affected postural control in the vestibulopathic state, trunk roll patterns in the head and earth-fixed water reward conditions were compared in both monkeys after vestibular ablation. For monkey M, the presence or absence of this sensory cue had only a small effect on RMS roll (Fig. 4). The increases in trunk roll seen for the foam conditions were perhaps due to the animal having to complete two tasks in the earth-fixed condition (i.e., stand on the platform and keep mouth affixed to tube) as opposed to the head-fixed condition (i.e., stand on the platform). Also, monkey M was already able to compensate for its vestibular loss without this added task/cue. In contrast, monkey S had *substantially less trunk roll* in three of the four platform configurations using the earth-fixed reward system (Fig. 4; two-sided t-tests: $p < 0.01$ for gum-wide, foam-narrow, and foam-wide).

http://dx.doi.org/10.1016/j.heliyon.2017.e00270

We further explored the effects of vestibular ablation with a quiet stance feedback controller model that probed if changes in intrinsic/short-latency muscle stiffness (in response to mild vestibular damage) and long-latency mechanisms (in response to severe vestibular damage) could adequately explain our experimental results. For the pre-ablated animal, the model yielded parameter values of K = 8 N*m/deg and B = 0.62 N*m*s/deg. The monkey damping was near that reported for humans, but the doubling in stiffness could be due to physiologic/anatomic differences between humans and monkeys, including differences in strength-to-weight ratios. Using similar procedures, K and B in the mildly ablated monkey were determined to be 12.5 N*m/deg and 1.47 N*m*s/deg, respectively. As model parameters K and B increased from the pre-ablated state, to the mildly ablated state (Fig. 5, top-left and top-middle), the simulated roll tilt decreased, mimicking the experimental data (Fig. 5, bottom).

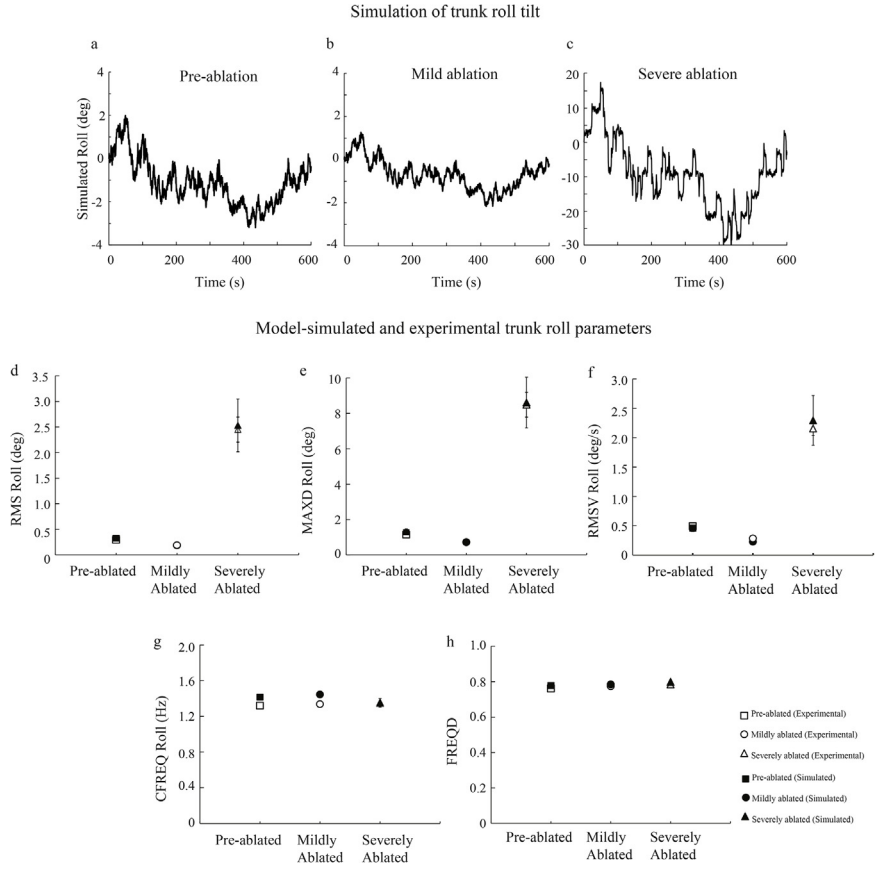

Fig. 5. *(Top)* Simulated trunk roll versus time for each of the three states for the foam-wide, head-fixed reward test condition. *(Bottom)* Comparison of motion parameters calculated from the experimental data (filled icons) and from the model simulations (open icons) in the three states. Pre-ablated and mildly ablated data are from monkey M and severely ablated data are from monkey S. Icons are means and error bars are standard error.

http://dx.doi.org/10.1016/j.heliyon.2017.e00270

For the severely ablated state, our model simulation and experimental results were most closely matched by shifting the parameters in the long-latency pathway (Fig. 2), K_p of 0.7 N*m/deg and a K_d to 0.02 N*m*s/deg, while keeping the intrinsic/short-latency at 0.4 N*m*s/deg. A sample of the simulated trunk roll that approximated the experimental data is shown in Fig. 5 (top-right). Model-simulated results closely matched the experimental measures (Fig. 5, bottom).

4. Discussion

In rhesus monkeys, mild vestibular damage is associated with a reduction in trunk roll while severe ablation results in increased trunk roll. Also, feedback controller models (previously only used to interpret human postural control) can quantify non-human primate trunk responses. Based on prior quiet stance studies in humans with severe bilateral vestibular hypofunction [7], we had predicted that mild and severe vestibular ablation would result in increased trunk roll. However, we observed either reductions/no change in trunk roll for the mildly ablated state and increases in trunk roll for the severely ablated state. To interpret these results, a quiet stance feedback controller model was utilized which demonstrated that increases in intrinsic/short-latency muscle stiffness (for mild vestibular damage) and long-latency mechanisms (for severe vestibular damage) could adequately explain our experimental results.

Peterka [18], and others (e.g., [28]), have suggested that intrinsic/short-latency ankle stiffness is very low and that long-latency stiffness plays a dominant role in postural responses. In contrast, other studies have suggested that the intrinsic/short-latency mechanisms are responsible for a large proportion of corrective torques required to maintain upright stance [25], [29, 30, 31]. Most relevant to the current study are the observations that intrinsic/short-latency stiffness is substantial for small, slow ankle rotations but decreases as the size of the ankle rotation increased [27], and that long-latency stiffness values are higher for bilateral vestibular-loss subjects than normal subjects [18]. Our experimental results showed that mild vestibular ablation resulted in a reduction in trunk roll and that the trunk roll may be reduced by intrinsic muscular/short-latency mechanisms that increase the body's rigidity. This mechanism is perhaps similar to the proposed increase in muscle stiffness in vestibulopathic subjects that allows them to achieve normative postural trunk roll when they perceive a threat that relates to balance control (e.g., [14]).

For the severe ablated state in monkey S, we observed increased trunk roll relative to the mildly ablated state (Fig. 3). Three possible scenarios were posed: a) there was a large increase in intrinsic/short-latency stiffness (i.e., monkey S attempted to apply a similar, but more exaggerated strategy than monkey M in its mildly ablated state) without a corresponding increase in intrinsic/short-latency damping thus

http://dx.doi.org/10.1016/j.heliyon.2017.e00270

leading to oscillatory behavior and increased trunk roll; b) there was very small intrinsic/short-latency stiffness and damping due to monkey S in its severely ablated state having an opposite postural response compared to the pre-ablated state and thus the animal was unable to compensate; or c) the severely ablated animal utilized an alternate strategy involving long-latency, neural feedback mechanisms due to the larger trunk rolls (and larger ankle stretches) present.

The first scenario seems the least likely in that oscillatory behavior of the trunk associated with an increase in stiffness is not physiologic. For monkey M in the pre-ablated and mildly ablated states, experimental values for CFREQ (pre-ablated: 1.415 +/− .021 Hz and post-ablated: 1.445 +/− .031 Hz) were not significantly different and likely independent of the (vestibular) state of the animal. The second scenario seems more likely in that severe vestibular ablated animals (as in Macpherson et al., 2007 [32]) exhibit opposite postural strategies when compared to control. However, the third hypothesis is most aligned with the previous discussion on small versus large (ankle) rotations. More specifically, due to the large ankle rotations in the severely ablated state, and hence large body trunk roll, monkey S was likely utilizing long-latency mechanisms. Our model-simulated results were in support of this hypothesis in that increases in long-latency mechanisms led to trunk roll parameters that were close to experimental values (Fig. 5). Although monkey S was applying neural feedback control mechanisms, it was not generating a large enough corrective torque to reduce trunk roll.

After vestibular ablation, monkey S behaved similarly to vestibulopathic humans: it used the postural reference provided by the “light touch” cue to stabilize its trunk [8], [33]. In contrast, monkey M did not use the additional sensory cue to reduce body trunk roll and muscle co-contraction may have been a sufficient postural compensation mechanism, even without the additional sensory cue. In summary, we have demonstrated differences in postural strategies utilized when peripheral vestibular damage is mild versus severe. These findings are encouraging in that animals, such as rhesus monkeys, could be used for future posture studies involving the compensation methods used for postural control, as well as for the development of invasive prostheses and rehabilitative methods that are not yet ready for human trials.

Declarations

Author contribution statement

Lara A. Thompson, Richard F. Lewis: Conceived and designed the experiments; Performed the experiments; Analyzed and interpreted the data; Contributed reagents, materials, analysis tools or data; Wrote the paper.

http://dx.doi.org/10.1016/j.heliyon.2017.e00270

Csilla Haburcakova: Conceived and designed the experiments; Performed the experiments; Contributed reagents, materials, analysis tools or data; Wrote the paper.

Funding statement

This work was supported by the National Institutes of Health (NIH) grant DC8362 to the Principal Investigator, Richard F. Lewis, and by NIH Grant T32 DC00038 which supported Lara A. Thompson.

Competing interest statement

The authors declare no conflict of interest.

Additional information

No additional information is available for this paper.

Acknowledgements

We thank Dr. Conrad Wall for advice on experimental design, and Drs. Adam Goodworth and James Lackner.

References

[1] Strategic Plan (FY 2006-2008) [Online], National Institute on Deafness and Other Communication Disorders, NIDCD, 2008. Accessed May 20, 2010 www.nidcd.nih.gov/StaticResources/about/plans/strategic/strategic06-08.pdf.

[2] F.B. Horak, Postural compensation for vestibular loss and implications for rehabilitation, Restor. Neurol. Neurosci. 28 (1) (2010) 57–68.

[3] F.B. Horak, J.M. Macpherson, Postural orientation and equilibrium, in Comprehensive Physiology, by R. S. Dow Neurological Sciences Institute Legacy Good Samaritan Hospital & Medical Center. Portland, OR, Am. Physiol. Soc. (1996) 255–292.

[4] L.A. Thompson, C.F. Haburcakova, R.F. Lewis, Vestibular ablation and a semicircular canal prosthesis affect postural stability during head turns, Exp. Brain Res. 234 (11) (2016) 3245–3257.

[5] M.W. Rogers, M.L. Mille, Lateral stability and falls in older people, Exerc. Sport Sci. Rev. 31 (4) (2003) 182–187. https://www.ncbi.nlm.nih.gov/pubmed/14571957.

http://dx.doi.org/10.1016/j.heliyon.2017.e00270

[6] F.B. Horak, C.L. Shupert, V. Dietz, G. Horstmann, Vestibular and somatosensory contributions to responses to head and body displacements in stance, Exp. Brain Res. 100 (1) (1994) 93–106.

[7] F.B. Horak, L.M. Nashner, H.C. Diener, Postural strategies associated with somatosensory and vestibular loss, Exp. Brain Res. 82 (1) (1990) 167–177.

[8] J.R. Lackner, P. DiZio, J. Jeka, F. Horak, D. Krebs, E. Rabin, Precision contact of the fingertip reduces postural trunk sway of individuals with bilateral vestibular loss, Exp. Brain Res. 126 (4) (1999) 459–466.

[9] P.C. Camana, H. Hemami, C.W. Stockwell, Determination of feedback for human postural control without physical intervention, Journal of Cybernetics 7 (3–4) (1977) 199–225.

[10] M. Cenciarini, P.J. Loughlin, P.J. Sparto, M.S. Redfern, Stiffness and damping in postural control increase with age, IEEE Trans. Biomed. Eng. 57 (2) (2010) 267–275.

[11] R. Johansson, M. Magnusson, Human Postural Dynamics, Crit. Rev. Biomed. Eng. 18 (6) (1991) 413–437. https://www.ncbi.nlm.nih.gov/pubmed/1855384.

[12] D.A. Winter, Human balance and posture control during standing and walking, Gait Posture 3 (4) (1995) 193–214. https://www.ncbi.nlm.nih.gov/pubmed/1855384.

[13] H. van der Kooij, R. Jacobs, B. Koopman, F. van der Helm, An adaptive model of sensory integration in a dynamic environment applied to human stance control, Biol. Cybern. 84 (2) (2001) 103–115.

[14] M.G. Carpenter, J.S. Frank, C.P. Silcher, G.W. Peysar, The influence of postural threat on the control of upright stance, Exp. Brain Res. 138 (2) (2001) 210–218.

[15] S.J. De Serres, T.E. Milner, Wrist muscle activation patterns and stiffness associated with stable and unstable mechanical loads, Exp. Brain Res. 86 (2) (1991) 451–458.

[16] P.L. Gribble, L.I. Mullin, N. Cothros, A. Mattar, Role of cocontraction in arm movement accuracy, J. Neurophysiol. 89 (5) (2003) 2396–2405.

[17] O. Missenard, L. Fernandez, Moving faster while preserving accuracy, Neuroscience 197 (1) (2011) 233–241.

[18] R.J. Peterka, Sensorimotor integration in human postural control, J. Neurophysiol. 88 (3) (2002) 1097–1118. http://jn.physiology.org/content/88/3/1097.full.

 http://dx.doi.org/10.1016/j.heliyon.2017.e00270

[19] L.B. Minor, Intratympanic gentamicin for control of vertigo in Meniere's disease: vestibular signs that specify completion of therapy, Am. J. Otol. 20 (2) (1999) 143–292.

[20] S.J. Judge, B.J. Richmond, F.C. Chu, Implantation of magnetic search coils for measurement of eye position: an improved method, Vision Res. 20 (6) (1980) 535–538. https://www.ncbi.nlm.nih.gov/pubmed/6776685.

[21] C. Maurer, R.J. Peterka, A New Interpretation of Spontaneous Trunk roll Measures Based on a Simple Model of Human Postural Control, J. Neurophysiol. 93 (1) (2005) 189–200.

[22] T.E. Prieto, J.B. Myklebust, R.G. Hoffman, E.G. Lovett, B.M. Myklebust, Measures of postural steadiness: differences between healthy young and elderly adults, IEEE Trans. Biomed. Eng. 43 (9) (1996) 956–966.

[23] M. Cenciarini, P.J. Loughlin, P.J. Sparto, M.S. Redfern, Stiffness and damping in postural control increase with age, IEEE Trans. Biomed. Eng. 57 (2) (2010) 267–275.

[24] A.D. Goodworth, R.J. Peterka, Influence of Bilateral Vestibular Loss on Spinal Stabilization in Humans, J. Neurophysiol. 103 (4) (2010) 1978–1987.

[25] D.A. Winter, A.E. Patla, F. Prince, M. Ishac, K.G. Percsak, Stiffness Control of Balance in Quiet Standing, J. Neurophysiol. 80 (3) (1998) 1211–1221. https://www.ncbi.nlm.nih.gov/pubmed/9744933.

[26] J.A. Vilenksy, Masses, Centers-of-Gravity, and Moments-of-Inertia of the Rhesus monkey (Macaca Mulatta), Am. J. Phys. Anthrop. 50 (1) (1979) 57–66.

[27] I. Loram, C. Maganaris, M. Lakie, The passive, human calf muscles in relation to standing: the non-linear decrease from short range to long range stiffness, J. Physiol. 584 (2) (2007) 661–675.

[28] X. Qu, N.A. Nussbaum, Evaluation of the roles of passive and active control of balance using a balance control model, J. Biomech. 42 (12) (2009) 1850–1855.

[29] V.S. Gurfinkel, M.I. Lipshits, S. Mor, K.E.T. Popov, The state of stretch reflex during quiet standing in man, Prog. Brain Res. 44 (1976) 473–486.

[30] L.M. Nashner, Adapting reflexes controlling the human posture, Exp. Brain Res. 26 (1) (1976) 59–72.

[31] I.D. Loram, M. Lakie, Direct measurement of human ankle stiffness during quiet standing: the intrinsic mechanical stiffness is insufficient for stability, J. Physiol. 545 (3) (2002) 1041–1053.

 http://dx.doi.org/10.1016/j.heliyon.2017.e00270

[32] J.M. Macpherson, D.J. Everaert, P.J. Stapley, L.H. Ting, Bilateral Vestibular Loss in Cats Leads to Active Destabilization of Balance During Pitch and Roll Rotations of the Support Surface, J. Neurophysiol. 97 (6) (2007) 4357–4367.

[33] J.R. Lackner, E. Rabin, P. DiZio, Stabilization of posture by precision touch of the index finger with rigid and flexible filaments, Exp. Brain Res. 139 (4) (2001) 454–464.

 http://dx.doi.org/10.1016/j.heliyon.2017.e00270